Modeling and simulation of a silicon soil moisture sensor based on the DPHP method for agriculture

A. Valente[1], R. Morais[1], C. Couto[2] and J. H. Correia[2]

[1]UTAD University, Dept. Engenharias, Quinta de Prados, 5000-911 Vila Real, Portugal
email: avalente@utad.pt   http://www.utad.pt/~aci
[2]University of Minho, Campus de Azurém, 4800-058 Guimarães, Portugal

Summary. A silicon soil moisture sensor, based in the dual-probe heat-pulse (DPHP) method, was modeled and simulated for achieving, with low cost, accurate and reliable measurements. This method is based on the application of a heat pulse during a fixed interval of time. The maximum rise in temperature ($\triangle T_m$) is monitored by the measurement probe, placed at a certain distance of the heater source. A low-cost high-performance and small temperature sensor (a dynamic V_{PTAT} generator) is required to be placed into the probe which have 0.912 mm in diameter and 20 mm long. If one considers the range of water contents, ratio of water mass to dry soil mass, in a typical agricultural soil (0.05 to 0.35 m^3 m^{-3}), the average sensitivity of the dual probe is about $1.95°C$ per unit change (m^3 m^{-3}) in water content for $q = 400$ Jm^{-1}.

Keywords: Soil moisture sensor, DPHP method, CMOS temperature sensor
Category: 1 (General,Theoretical and modeling)

1 Introduction

Efficient short and long-term management of irrigation systems requires the use of reliable and accurate soil moisture sensors. Today, a large number of sensors, based on nuclear, electromagnetic, tensiometric, capacitance, among others, techniques are available for measuring soil moisture. Generally, these methods have several limitations that restrict their integration in the management of irrigation systems. The main disadvantages are: soil dependency, inaccuracy and high-cost sensors.

Time domain reflectometer (TDR) sensors [1, 2], which are based on the influence of soil water content over the propagation of electromagnetic waves, are independent of soil texture, temperature and salt content, but its high cost restricts the applicability to these systems.

Therefore, the development of a low-cost miniaturized system with electronics, network solution, and external communications that could be implemented next to the plant roots will be a breakthrough. The same basic fabrication concepts and materials, which have made microelectronics successful, are now being adapted to making low-cost, small, high-performance sensor systems devices, e.g. a silicon soil moisture sensor.

The dual-probe heat capacity sensor has been developed to provide small scale, frequent measurements of soil thermal properties: volumetric heat capacity (ρc_p), thermal conductivity, and thermal diffusivity. The heat capacity of soil influences both the storage and transfer of heat, so it is a necessary parameter in models of soil temperature and heat flow. In a nonswelling soil, changes in ρc_p are due primarily to changes in soil water content; hence, an application of the dual-probe is to allow determination of volumetric soil water content (θ_v) [3, 4].

The dual-probe heat-pulse (DPHP) sensor is about $30mm$ long $\times 6mm$ wide $\times 0.8mm$ in height; the probe pitch is $3mm$ for allowing small-scale spatial measurements of soil moisture, which can be made near the soil surface where large root densities are found.

2 Theory

The heat capacity of soil, ρc_p, is evaluated by adding the volumetric heat capacities of soil constituents:

$$\rho c_p = 1.92X_m + 2.51X_o + 4.18\theta_v \qquad (1)$$

where X_m, X_o, and θ_v are the mineral, organic, and water fractions of the soil, respectively. The leading coefficients represent the volumetric heat capacity ($MJm^{-3°}C^{-1}$) of each soil constituent. When a pulse of heat is applied during a fixed interval of time to the heater probe, the maximum rise in temperature ($\triangle T_m$) at some distance from the heater is measured. As mentioned by Campbell *et al.* [5] the relationship between the ρc_p and $\triangle T_m$ is,

$$\rho c_p = \frac{q}{e\pi r^2 \triangle T_m} \qquad (2)$$

where, q (Jm^{-1}) is the heat applied per unit length of the heater, e is the base of natural logarithms, and

$r(m)$ is the distance between the heat and temperature probes. Substituting Eq. 1 into Eq. 2 and rearranging yields an expression that shows the relationship between θ_v and $\triangle T_m$,

$$\triangle T_m = \frac{q}{e\pi r^2(1.92X_m + 2.50X_o + 4.18\theta_v)} \quad (3)$$

or,

$$\theta_v = \frac{\frac{q}{e\pi r^2 \triangle T_m} - (1.92X_m + 2.50X_o)}{4.18} \quad (4)$$

Although $\triangle T_m$ varies with ρc_p and θ_v, q can be selected to produce an adequate temperature signal for the expected range of θ_v for a typical agricultural soil (0.05 to $0.35\ m^3m^{-3}$).

From a oven–dry to saturated soil, $\triangle T_m$ varies by only about $1.2°C$; therefore, accurate measurements of $\triangle T_m$ are required to correctly estimate θ_v. Taking the partial derivative of $\triangle T_m$ with respect to θ_v yields the sensitivity of temperature rise to the change in soil water content:

$$\frac{\partial \triangle T_m}{\partial \theta_v} = \frac{-4.18q}{e\pi r^2(1.92X_m + 2.50X_o + 4.18\theta_v)} \quad (5)$$

If one considers the range of water contents in a typical agricultural soil, the average sensitivity of the dual-probe is about $2.5°C$ per unit change (m^3m^{-3}) in water content; that is, a 1% change in θ_v cause a $0.025°C$ change in $\triangle T_m$.

3   Projected system

The system consists of two needle probes mounted in parallel to provide a heater and a sensor probe. The needles will be made from stainless steel tubing, $0.912mm$ in diameter, which will protrude $20mm$ beyond the edge of the acrylic mounting [6].

The heater will be made from Stablohm 800A wire and placed in the middle of 'heater' needle. A high-accuracy CMOS temperature sensor with amplifier will be placed in the center of the 'probe' needle. The needles will be filled with high-thermal-conductivity epoxy glue to provide water-resistant, electrically insulated probes. The complete projected system is illustrated schematically in Fig. 1.

4   Heat-pulse simulations

Experimentally, it is not possible to heat the line source instantaneously, so a short-duration heat pulse is used. Fig. 2 shows the calculated temperatures at a distance r following application of equivalents amounts of energy via instantaneous and short-duration heat pulses. The short-duration heat pulse causes a significant delay in
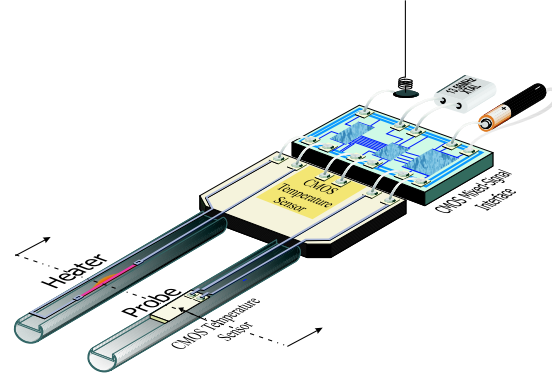

Fig. 1: The complete soil moisture sensor system.

time at which the maximum temperature change is obtained, but has very little effect on $\triangle T_m$. Because of this minimal effect on $\triangle T_m$, it is possible to use the instantaneous theory with short-duration heat pulses to obtain accurate heat capacities, and hence soil moisture.
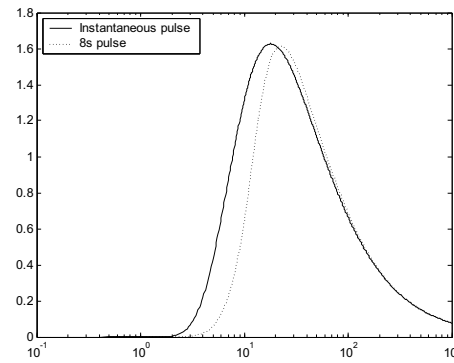

Fig. 2: Simulated temperature for instantaneous and pulsed line source models.

For a given θ_v, the sensitivity of $\triangle T_m$ increases as more energy is applied to the probe (q), but decreases with larger probe spacing and higher bulk densities. The $\triangle T_m$ distribution were simulated, using FEMLAB, and the Fig. 3 shows these results.
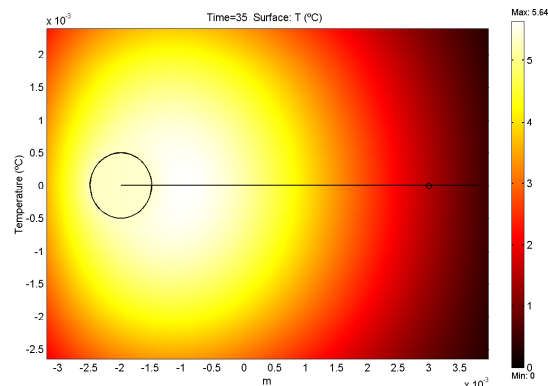

Fig. 3: Simulated $\triangle T_m$ distribution at $35s$.

5 Temperature sensor simulations

A low-cost, small and high-performance temperature sensor is required to be placed in a stainless steel needle with $0.912mm$ in diameter and $20mm$ long. A proportional to absolute temperature (PTAT) circuit with bipolar devices fabricated in the CMOS process meet these criteria. Meijer *et al.* [7] showed that the application of dynamic voltage processing, using dynamic element matching (DEM) and dynamic amplification, will enable to get a very high performance temperature sensor.

The high-performance CMOS temperature sensor is composed of a dynamic V_{PTAT} generator with thirty two switching stages. This technique is depicted in Fig. 4 were transistors $M_1 - M_{16}$ represent sixteen current mirrors. One of these transistors supplies current to the bipolar transistor Q_1 while the other fifteen supply current to Q_2, so that the current (I_{c2}) passing through Q_2 is fifteen times the current (I_{c1}) passing through Q_1.

The difference between the base-emitter voltages V_{BE2} and V_{BE1} represents the PTAT voltage. Next, using switches, the positions of $M_1 - M_{16}$ are cyclically interchanged. After a complete cycle the averaged results represent a PTAT voltage in which the effect of any mismatch in the characteristic of the transistors $M_1 - M_{16}$ is strongly reduced. In order to eliminate the mismatch in the transistors Q_1 and Q_2 their relative positions are interchanged as well. So, a complete cycle consists of thirty two sub-cycle states producing an average value of V_{PTAT} over these states almost equal to $(nkT/q)\ln 15$ (Fig. 5).
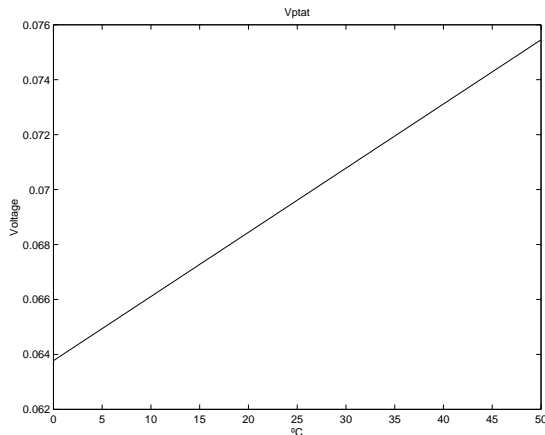

Fig. 5: Simulated PTAT voltage.

The PTAT voltage over a sub-cycle is amplified using a dynamic switched capacitor amplifier with a DC gain of fifteen. The Fig. 6 shows half of the DEM amplifier. The DEM technique is realized by sequentially changing the relative positions of the capacitors each clock cycle. In each clock cycle, one of the identical capacitors $C_1 - C_{16}$ is in the feedback position (C_F) and all the others are in the input position (C_I). The

average value of the amplification factor in a complete cycle is equal to $G = \frac{C_I}{C_F} = 15$ where the effect of capacitor mismatching is almost eliminated.
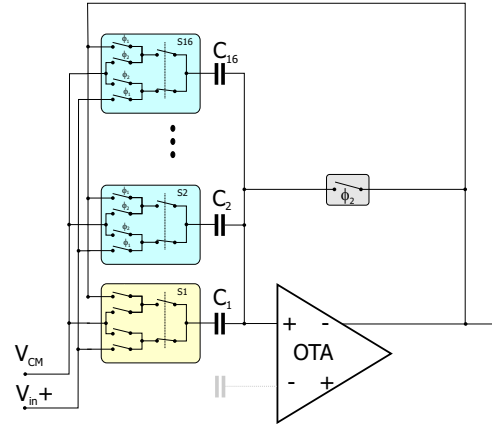

Fig. 6: Half schematic of the DEM amplifier.

The average of the gain in a complete cycle equals to

$$\overline{G} = \frac{1}{G+1} \sum_{i=1}^{G+1} \frac{\sum_{j=1}^{G+1} C_i - C_j}{C_i} = G + \triangle G. \quad (6)$$

Where $\triangle G$ represents the residual second order error of the mismatching.

Using dynamic PTAT generator and dynamic switched capacitor amplifier will enable to get a very high performance temperature sensor. Using these techniques, even without trimming or adjustment and even when using low-cost inaccurate components, a high precision of an amplifier-gain factor is obtained.

The fig. 7 shows the layout of the CMOS temperature sensor. Simulations performed using values from this layout indicates a sensor sensitivity of about $3.5mV °C^{-1}$ or $6.825mV$ per unit change ($m^3 m^{-3}$) in water content for a heat strength of $400Jm^{-1}$.
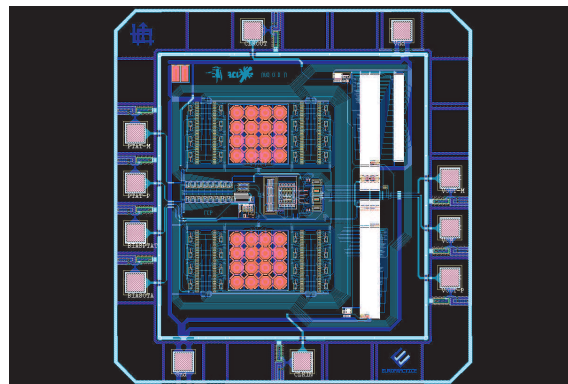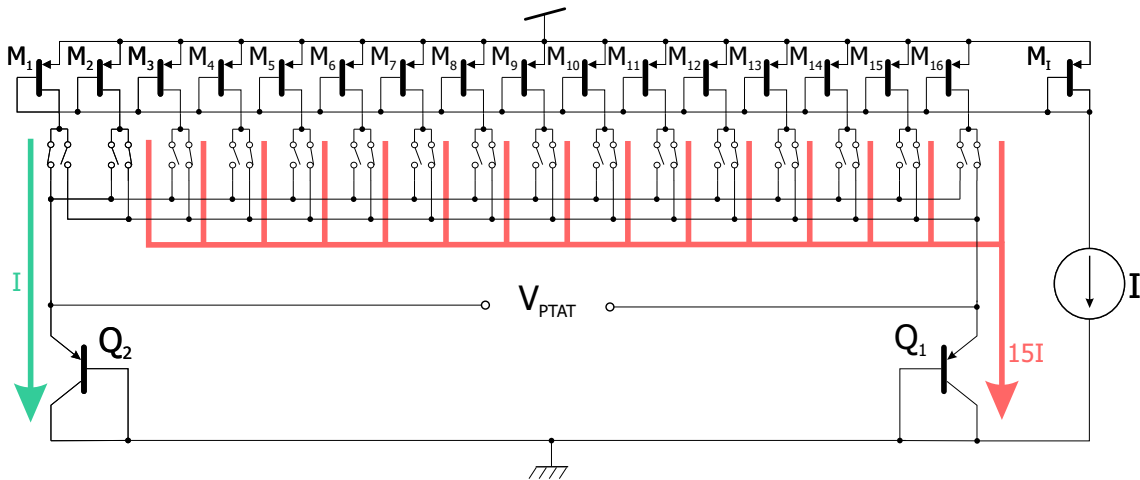

Fig. 7: Temperature sensor layout.

Fig. 4: Generation of V_{PTAT} using DEM, according to [7]

6 Conclusions

The modeling and simulation of a soil moisture sensor using the dual-probe heat-pulse method were achieved. Simulations shown that an accurate PTAT voltage can be generated with the implementation of dynamic element matching techniques. With the application of the same concept to the amplifier, the effect of the component mismatching has been eliminated significantly.

It is also shown that the sensitivity of the dual probe is about $1.95°C$ per unit change ($m^3\ m^{-3}$) in water content for a heat strength of q of $400\ Jm^{-1}$.

References

[1] C. G. Topp, J. L. Davis and A. P. Annan (1980). Electromagnetic determination of soil water content using TDR: Measurements in coaxial transmission lines, *Water Resour. Res.*, **16** (1980) 574–582.

[2] C. G. Topp, J. L. Davis. Measurement of soil water content using time-domain reflectometry (TDR): A field evaluation, *Soil Sci. Soc. Am. J.*, **49** (1985) 19–24.

[3] Julie M. Tarara and Jay M. Hamm. Measuring soil water content in the laboratory and field with dual-probe heat-capacity sensors. *Agronomy Journal*, **89** (1997) 535–542.

[4] Y. Song, J. H. Hamm, M. B. Kirkham and G. J. Kluitenberg. Measuring soil water content under turfglass using the dual-probe heat-pulse technique. *J. Amer. Soc. Hort. Sci.*, **123(5)** (1998) 937–941.

[5] G. S. Campbell, C. Calissendorff and J. H. Williams. Probe for measuring soil specific heat using heat-pulse method. *Soil Sci. Soc. Am. J.*, **55** (1991) 291–293.

[6] A. Valente, J. Boaventura Cunha and C. Couto. Soil Moisture Sensor with Built-in Fault-detection Capabilities. *Proc. of 24th Anual Conf. of IEEE Ind. Electronics Society*, Aachen, Germany, August 31–September 4, (1998) 1310–1314.

[7] G. C. M. Meijer, G. Wang, F. Fruett. Temperature Sensors and Voltage References Implemented in CMOS Technology. *IEEE Sensors Journal*, **1(3)** (2001) 225–234.